Inorganic Fullerene Nanoparticles

Fullerene-Like Rare-Earth Nanoparticles**

*Xun Wang and Yadong Li**

The landmark discovery of the fullerenes[1] has led to the development of thermodynamically stable forms of carbon whose dimensions are reduced to the nanoscale.[1–2] As an analogue to these novel structures, the concept of inorganic fullerene-like (IF) nanostructures has been initially described and confirmed by Tenne and co-workers.[3–6] Stimulated by the novel properties of fullerenes,[7–8] these IF nanoparticles can be expected to open new avenues in the solid-state chemistry of inorganic compounds and offer new opportunities for the application of such nanostructures in the emerging field of nanotechnology, as well as in numerous other areas.[9–12] However, up to now, only a limited number of IF nanoparticles have been successfully prepared from their corresponding layered inorganic compounds, such as WS_2,[3] MoS_2,[5] $NiCl_2$,[6] $CdCl_2$,[13] Tl_2O,[14] NbS_2,[15] and ReS_2.[16] The synthesis of novel IF nanoparticles remains as a challenging task for the years to come. Herein we report the synthesis of rare-earth fluoride and hydroxide IF nanoparticles using a low-temperature hydrothermal synthetic procedure.

In contrast to nanotubes, the formation of IF particles requires folding in all directions, and thus involves higher elastic strain.[9–10] Generally, the synthesis of inorganic fullerene-like particles does not need a catalyst, but usually requires relatively high temperatures.[9] The techniques by which the high temperatures have been achieved includes furnaces,[3,5,6,16] laser vaporization,[1] sonolysis,[14] electron and ion-beam heating,[13] and heating by an STM tip.[17] In this paper, a rational hydrothermal synthetic procedure has been successfully developed to prepare rare-earth IF hollow nanoparticles at low temperatures (80–180 °C), which may suggest a route for the future exploration of synthetic procedures to new IF nanostructures. It is also worthy to note that the fluorides and hydroxides of IF nanotructures have been obtained for the first time; previously, this has been limited to chloride and chalcogenides over the past decade. In addition, the novel properties of rare-earth compounds[18] makes them rather appealing for practical applications in, for example, luminescence, catalysis, and biological fields.

Our synthesis is based on a facile hydrothermal method. A typical synthesis involves the preparation of colloidal fluoride precipitates and/or mixtures of rare-earth oxides and water, which is then treated at a designated temperature under hydrothermal conditions.

The phase purity of the samples has been characterized on a Bruker D8-Advance X-ray powder diffractometer with $Cu_{K\alpha}$ radiation ($\lambda = 1.5418$ Å). Under the adopted conditions, the obtained LaF_3, PrF_3, NdF_3, and SmF_3 IF nanostructures all have hexagonal structures while YF_3 has an orthorhombic structure (Figure 1 d). As an example, Figure 1 a–c shows typical reflection patterns of LaF_3 IF nanoparticles obtained at a temperature of 120, 140, and 180 °C, respectively, which

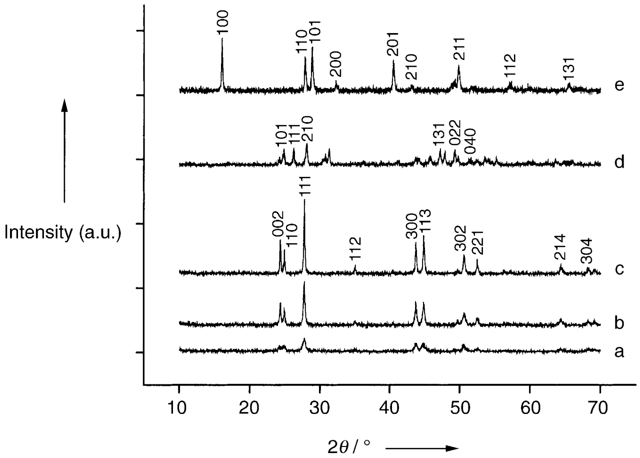

Figure 1. XRD patterns of a) LaF_3 IF nanoparticles (120 °C, La^{3+}:NH_4F = 1:3, pH 4–5); b) LaF_3 IF nanoparticles (140 °C, La^{3+}:NH_4F = 1:3, pH 4–5); c) LaF_3 IF nanoparticles (180 °C, La^{3+}:NH_4F = 1:3, pH 4–5); d) YF_3 IF nanoparticles (180 °C, Y^{3+}:NH_4F = 1:3, pH 4–5); e) $Nd(OH)_3$ nanotubes and IF nanoparticles (140 °C).

---

[*] Prof. Dr. Y. Li, X. Wang
Department of Chemistry
Tsinghua University
Beijing, 100084 (P. R. China)
Fax: (+86) 10-6278-8765
E-mail: ydli@tsinghua.edu.cn

[**] This work was supported by the NSFC (20025102, 50028201, 20151001), the Foundation for the Author of National Excellent Doctoral Dissertation of P. R. China, and the State Key Project of Fundamental Research for nanomaterials and nanostructures.

DOI: 10.1002/ange.200351006

can be readily indexed to that of the hexagonal phase of LaF_3 (JCPDS no. 72–1435) with lattice constants $a = 7.163$ and $c = 7.329$ Å. With decreasing hydrothermal temperature, the peaks have been apparently broadened (Figure 1a), which indicates smaller crystal sizes. It seems that the formation of IF nanoparticles is closely related to the hexagonal structures of the corresponding samples, since comparatively fewer IF nanoparticles have been observed in the samples of orthorhombic YF_3 and no IF nanostructures observed in the orthorhombic samples of other LnF_3 (Ln = Eu, Gd, Tb, Dy, Ho, Er, Tm, Yb, and Lu) under our experimental conditions. Similar to the fluorides, most of the hydroxide IF nanoparticles that have been examined possess hexagonal structures, which also coincides well with that of rare-earth hydroxide nanowires and nanotubes.[19–20] As an example, Figure 1e shows the diffraction pattern for $Nd(OH)_3$, which can be readily indexed to that of the hexagonal structure of $Nd(OH)_3$ (JCPDS no. 83-2035) with lattice constants $a = 6.418$ and $c = 3.743$ Å. A thorough XRD characterization indicates that pure phase of the rare-earth fluorides and hydroxides could be obtained under the reported experimental conditions.

Transmission electron microscopy (TEM) provides further insight into the morphology and microstructural details of the rare-earth-based series of IF nanostructures. Figures 2–4 shows typical images of these rare-earth compounds IF nanoparticles, from which it can be seen that most of the samples dispersed on the copper TEM grids have hollow-sphere morphologies.

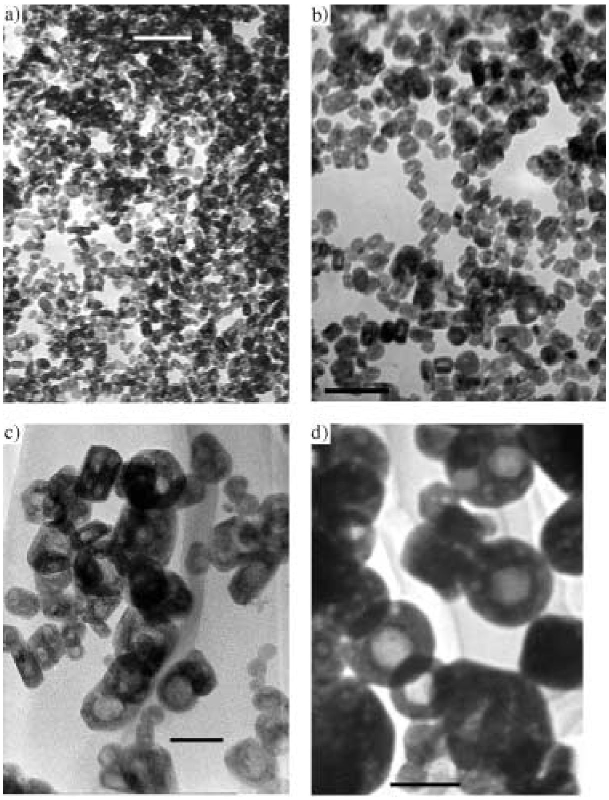

Figure 2. TEM images of a) LaF_3 IF nanoparticles (120 °C, La^{3+}:NH_4F = 1:3, pH 4–5); b) LaF_3 nanoparticles (140 °C, La^{3+}:NH_4F = 1:3, pH 4–5); c) LaF_3 nanoparticles (180 °C, La^{3+}:NH_4F = 1:3, pH 4–5); d) LaF_3 nanoparticles (180 °C, La^{3+}:NH_4F = 1:9, pH 4–5).

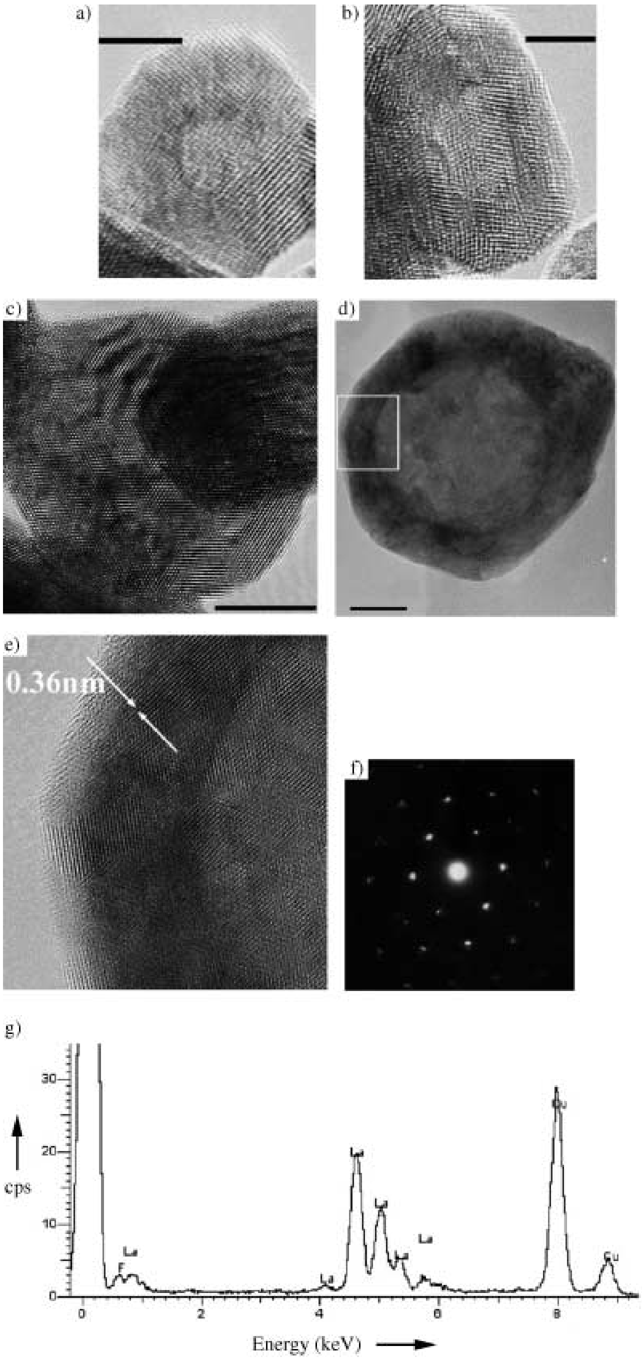

Figure 3. HRTEM images of a) an individual IF nanoparticle with diameter ≈10 nm; b) an individual polyhedral IF nanoparticle; c) an individual IF nanoparticle with diameter ≈30 nm; d) an individual IF nanoparticle with diameter ≈90 nm; e) Magnification of the square section shown in d); f) electron diffraction pattern of the IF nanoparticle in d); g) EDS analysis of the IF nanoparticle in d).

The sizes of these IF nanoparticles are flexible to some extent; temperature and molar ratio have been found to be responsible for the size and shape control of these nanostructures. As shown in Figure 2c and d, the size of the LaF_3

nanoparicles shrinks from approximately 100 to 30 nm when the molar ratio (La^{3+}:F^-) changes from 1:9 to 1:3. Temperature also plays an important role in determining the sizes of these IF nanostructures. Figure 2a shows that the average diameters of the LaF_3 obtained at 120 °C are approximately 10 nm, while at higher temperatures (140 °C and 180 °C), the average sizes increase to 20–40 and 30–50 nm, respectively.

Similar IF structures and size-control phenomena have been observed in the samples of PrF_3, NdF_3, and SmF_3, however, comparatively fewer IF nanoparticles have been observed in the samples of YF_3, perhaps due to its orthorhombic structure.

High-resolution (HR)TEM analysis provides more detailed structural information on these IF nanostructures, and a series of HRTEM images of LaF_3 nanoparticles with diameters ranging from 10 to 100 nm have been provided as further evidence for the formation of rare-earth fluoride IF nanostructures. Figure 3d shows an individual close-caged particle with a diameter of approximately 90 nm. Higher magnification shows that its wall contains about forty layers (Figure 3e). The interlayer distance is calculated to be approximately 0.36 nm (the separation between (002) planes). Electron diffraction (ED) analysis (Figure 3f) taken from this hollow nanoparticle has revealed its single-crystalline nature, and indicates that the nanoparticles have hexagonal symmetry. Energy-dispersive spectroscopy (EDS) of this nanoparticle indicates that it contains only La and F (Figure 3g). IF nanostructures of LaF_3 with different shapes and sizes have been shown in Figure 3a–c, from which the close-caged structures of these nanoparticles can be clearly discerned.

IF nanostructures have also been discovered in our rare-earth hydroxide samples. In contrast to the fluoride IF nanoparticles, the hydroxide nanoparticles usually coexist with nanotubes in the final product (for example in, $Y(OH)_3$, $Sm(OH)_3$, $Eu(OH)_3$, $Gd(OH)_3$, $Tb(OH)_3$, $Dy(OH)_3$, $Ho(OH)_3$, and $Er(OH)_3$). Figure 4 shows HRTEM images of an individual $Eu(OH)_3$ IF nanoparticle. The interlayer distances of the IF particles are approximately 0.364 nm (close to the lattice constant along the *c* axis of the $Eu(OH)_3$ structure). This value is in good agreement with that of the nanotubes obtained by another precipitation method.[20]

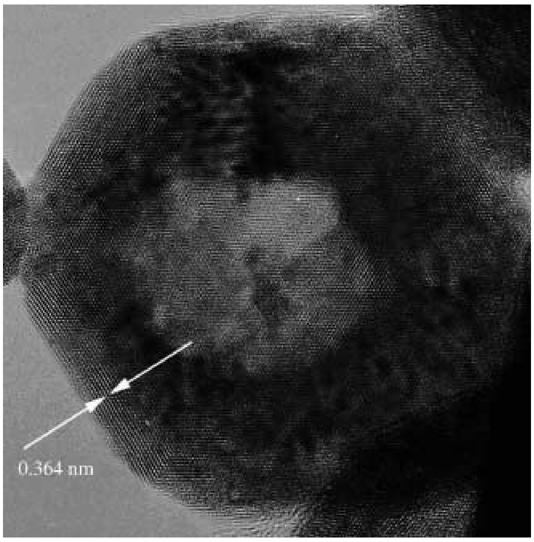

Figure 4. HRTEM image of an individual $Eu(OH)_3$ IF nanoparticle with diameter ≈45 nm.

The hollow-sphere nature of these samples has been further confirmed through Brunauer–Emmett–Teller (BET) analysis. Nitrogen adsorption/desorption isotherms and corresponding Barrett–Joyner–Halenda (BJH) pore-size distribution plots for samples of PrF_3 IF nanoparticles are shown in Figure 5. The isotherms can be categorized as type IV with a distinct hysteresis loop observed in the range of 0.6–1.0 P/P_0 (Figure 5a) for the samples at 120 °C, and 0.8–1.0 P/P_0 (Figure 5b) for the samples at 180 °C. The BET surface area for samples prepared at 180 °C (average diameters: 30–50 nm) and 120 °C (average diameters: about 10 nm) were 23.56 and 58.03 m^2g^{-1}, respectively; these values are much larger than the calculated value for monodisperse PrF_3 spherical nanoparticles (43.92, 21.96, 14,64, 10.98, and 8.78 m^2g^{-1} for spherical particles with diameters of 10, 20, 30, 40, and 50 nm, respectively; density of a single crystal of $PrF_3 = 6.83\ g\,cm^{-3}$) that are not hollow. The BJH calculations for the pore-size distribution based on desorption data reveal

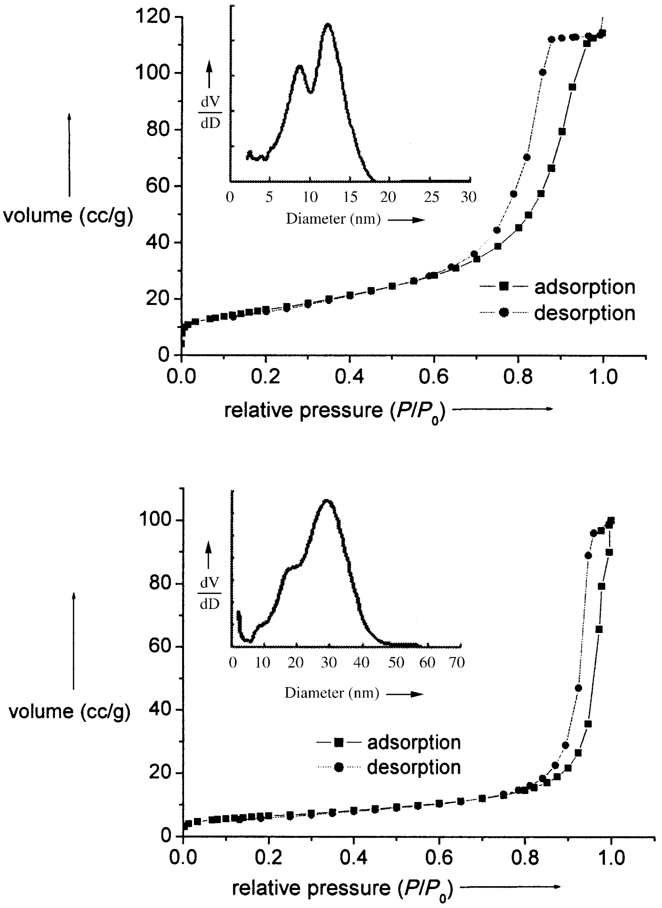

Figure 5. a) N_2 adsorption/desorption isotherm of PrF_3 IF nanoparticles (120 °C, Pr^{3+}:F^- = 1:3); inset, pore-size distribution curve obtained from the desorption data; b) N_2 adsorption/desorption isotherm of PrF_3 IF nanoparticles (180 °C, Pr^{3+}:F^- = 1:3); inset, pore-size distribution curve obtained from the desorption data.

a bimodal distribution for the 120 °C samples centered at 8.5 and 12 nm (Figure 5 a, inset), and a distribution for the 180 °C samples centered at 30 nm (Figure 5 b, inset), which coincides with the XRD and TEM results of the samples.

Compared with the reported IF nanostructures, rare-earth fluorides and hydroxides have no typical layer structures. However, it seems that the closed-cage structures are also thermodynamically stable for these fluorides and hydroxides. Based on our experimental results, single-crystal nanotubes of rare-earth hydroxides have been successfully obtained,[20] which have shown the possibility of hydroxides forming closed-cage structures. Meanwhile, in the process of studying the formation mechanism of rare-earth hydroxides nanowires, we have observed the wide existence of lamellar structures.[19] Similar two-dimensional (2D) growth phenomena have also been observed in the formation process of fluoride nanostructures. Therefore, we believe that the rare-earth fluorides and hydroxides may not be regarded as typical 3D compounds, and may be the structural intermediates between 3D and 2D structures. However, a clear explanation of the structural rational of these IF nanostructures may need a thorough theoretical and structural investigation.

In this paper, based on a low-temperature hydrothermal method, a series of rare-earth fluoride and hydroxide IF nanoparticles have been successfully synthesized, which have greatly extended the scope of IF nanostructures. Meanwhile, this facile procedure can be easily adjusted for the large-scale synthesis of rare-earth IF nanoparticles. Also, the studies have illustrated the potential of this solution-based route for the synthesis of IF nanostructures in the low-temperature range, especially for the layered hydroxides. We believe that the synthesis and the subsequent properties obtained from these IF structures will offer many opportunities in a number of areas.

Experimental Section

Synthesis of LnF_3 IF nanoparticles: In a typical synthesis, Ln_2O_3 (Y_2O_3, La_2O_3, Pr_2O_3, Nd_2O_3, Sm_2O_3; 0.4 g) was first dissolved in 10% nitric acid, then mixed with another solution containing NH_4F (molar ratio, Ln^{3+}:$F^{-}=1$:3) to form colloidal precipitates. 10% KOH (or NaOH) was then added to adjust the system to pH 4–5. The obtained colloidal precipitate was transferred to a 40-mL autoclave, sealed, and maintained at 80–180 °C for 12–24 h; the autoclave was then allowed to cool to room temperature. The precipitate was then filtered, washed with water to remove ions possibly remnant in the final products, and dried at 80 °C in air. Following the above procedures, IF nanoparticles of LaF_3, PrF_3, NdF_3, SmF_3 and YF_3 could be easily obtained. In order to obtain IF nanostructures with different sizes, factors such as molar ratio and temperature have been varied during the experimental process. The functionalization process could also be easily carried out by dissolving the corresponding rare-earth oxides with target ions or atoms.

Synthesis of $Ln(OH)_3$ IF nanoparticles: In a typical synthesis, rare-earth oxide powders (La_2O_3, Pr_6O_{11}, Nd_2O_3, Sm_2O_3, Eu_2O_3, Gd_2O_3, Tb_4O_7, Dy_2O_3, Ho_2O_3, Er_2O_3, Y_2O_3; 0.4 g) were dispersed into distilled water (30 ml), then sealed in a 40-mL autoclave and hydrothermally treated at 140–180 °C for 24 h.

Characterization: The obtained sample was characterized on a Bruker D8-Advance X-ray powder diffractometer with $Cu_{K\alpha}$ radiation ($\lambda = 1.5418$ Å). The size and morphology of the IF nanoparticles were determined at 200 kV by a Hitachi H-800 transmission electron microscope (TEM) and a JEOL JEM-2010F high-resolution transmission electron microscope.

Received: January 23, 2003 [Z51006]

Keywords: fluorides · fullerenes · hydroxides · nanostructures · rare-earth metals

---

[1] H. W. Kroto, J. R. Heath, S. C. O'Brien, R. F. Curl, R. E. Smalley, *Nature* **1985**, *318*, 162–163.
[2] S. Iijima, *Nature* **1991**, *354*, 56–58.
[3] R. Tenne, L. Margulis, M. Genut, G. Hodes, *Nature* **1992**, *360*, 444–446.
[4] L. Margulis, G. Salltra, R. Tenne, M. Tallanker, *Nature* **1993**, *365*, 113–114.
[5] Y. Feldman, E. Wasserman, D. J. Srolovitz, R. Tenne, *Science* **1995**, *267*, 222–225.
[6] Y. R. Hacohen, E. Grunbaum, R. Tenne, J. Sloan, J. L. Hutchison, *Nature* **1998**, *395*, 336–337.
[7] M. Prato, M. Maggini, *Acc. Chem. Res.* **1998**, *31*, 519–526.
[8] A. L. Balch, M. M. Olmstead, *Chem. Rev.* **1998**, *98*, 2123–2165.
[9] R. Tenne, *Prog. Inorg. Chem.* **2001**, *50*, 269–315.
[10] R. Tenne, *Chem. Eur. J.* **2002**, *8*, 5297–5304.
[11] G. L. Frey, S. Elani, M. Homyonfer, Y. Feldman, R. Tenne, *Phys. Rev. B* **1998**, *57*, 6668–6671.
[12] M. Chowalla, G. A. J. Amaratunga, *Nature* **2000**, *407*, 164–167.
[13] R. Popovitz-Biro, A. Twersky, Y. R. Hacohen, R. Tenne, *Isr. J. Chem.* **2001**, *41*, 7–14.
[14] S. Avivi, Y. Mastai, A. Gedanken, *J. Am. Chem. Soc.* **2000**, *122*, 4331–4334.
[15] C. Schuffenhauer, R. Popovitz-Biro, R. Tenne, *J. Mater. Chem.* **2002**, *12*, 1587–1591.
[16] K. S. Coleman, J. Sloan, N. A. Hanson, G. Brown, G. P. Clancy, M. Terrones, H. Terrones, M. L. H. Green, *J. Am. Chem. Soc.* **2002**, *124*, 11580–11581.
[17] M. Homyonfer, Y. Mastai, M. Hershfinkel, V. Volterra, J. L. Hutchison, R. Tenne, *J. Am. Chem. Soc.* **1996**, *118*, 7804–7808.
[18] G. X. Xu, *Rare Earths*, 2nd ed., Metallurgical Industry Press, Beijing, **1995**.
[19] X. Wang, Y. D. Li, *Angew. Chem.* **2002**, *114*, 4984–4987; *Angew. Chem. Int. Ed.* **2002**, *41*, 4790–4793.
[20] "Rare earth compound nanotubes": X. Wang, Y. D. Li, unpublished results.